# Transient Simulations and Analyses of Thermally Tunable Devices

Fei Duan, Kai Chen, Yonglin Yu
Wuhan National Laboratory for Optoelectronics, Huazhong University of Science and Technology, Wuhan, China
*Email: yonglinyu@mail.hust.edu.cn; feiduan@hust.edu.cn

***Abstract*— we present transient simulations and analytic formulas for the thermally tunable devices with suspended waveguide. The response speeds can be improved about 10% and 40%, when the thickness of metallic heater varies from 0.08 µm to 0.16 µm and the cladding thickness increases from 0.4 µm to 1.2 µm, respectively. Moreover, replacing the cladding of silica by ones of Alumina, aluminum nitride and silicon nitride, the response speed have a significant boost, more than 65%.**

***Keywords—thermally tunable device, response speed, transient simulation, filters, switches***

## I. Introduction

Thermally tunable devices, such as thermally tunable filters and switches, are becoming ones of the most popular options for reconfigurable photonics devices [1]. Among these devices, waveguide grating and Mach-Zehnder interferometer (MZI) structures are widely used currently. Furthermore, suspended waveguide structures for thermally tunable grating filters and MZI switches have been proposed to reduce the power consumption, improving the tuning efficiency of the devices [2-4]. However, the thermal isolation between the waveguide and substrate results in significant decrease in the response speed [4, 5].

In this paper, based on our previous works [6], we present transient simulation and analytic formulas to study the temperature response process of these thermally tunable devices. Results show that the response speed of the devices can be optimized with the layer thickness and the cladding materials.

## II. Design and Simulation

### A. Device Design and Structure

Thermally tunable filter and switch are schematically shown in Fig. 1 (a) and (b) separately. In order to increase the tuning efficiency, the grating section of filter and tuning section of switch are designed as the suspended waveguide structure with laterally sustained beam and pillar as illustrated in Fig. 1 (c). Through the beam and $SiO_2$ (silica) pillar, the heater, cladding and Si (silicon) waveguide has indirect contact with the Si substrate. The metallic heater is made up of gold (Au) and titanium (Ti), while the cladding can be deposited by $SiO_2$, alumina ($Al_2O_3$), aluminum nitride (AlN) and silicon nitride ($Si_3N_4$). The thicknesses and properties of these materials are listed in Table I [7-11]. The parameters of beam and pillar structures are the same as previously proposed case in [5].

TABLE I. Dimensional and Physical Parameters of Materials

| Material | $\delta$ (nm) | $\rho$ (kg/m$^3$) | $C_p$ (J/(kg·°C)) | $k$, (W/(m·°C) | $\sigma_0$ ($10^{-9}$ Ω·m) |
|---|---|---|---|---|---|
| Au | 160 | 19300 | 130 | 317 | 22.14 |
| Ti | 40 | 4510 | 575 | 14.6 | 420 |
| Si [7] | 220 | 2329 | 700 | 60 | / |
| $SiO_2$ [8] | 800 | 2203 | 966 | 1.0 | / |
| $Al_2O_3$ [9] | 1000 | 3970 | 780 | 40 | / |
| AlN [10] | 1000 | 3300 | 820 | 50 | / |
| $Si_3N_4$ [11] | 1000 | 2500 | 170 | 14 | / |

*$\delta$, $\rho$, $C_p$, $k$, $\sigma_0$ are film thickness, density, specific heat capability, heat conduction coefficient, electric resistivity at room temperature, respectively.

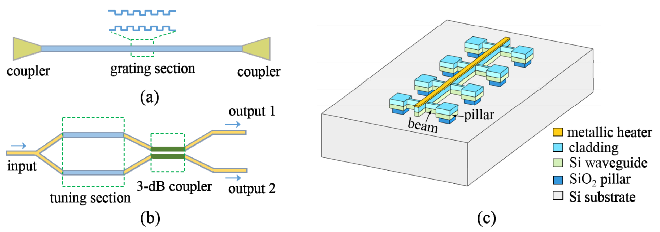


Fig. 1. Schematic of the thermally tunable devices (a) filter, (b) MZI switch and (c) suspended waveguide structure

### B. Transient Model and Analytic Formulas

To simulate the temperature distribution and response speed, the transient model of heat transfer in COMSOL Multiphysics software is selected as [12]

$$\rho C_p \frac{\partial T}{\partial t} - K \cdot \nabla^2 T = Q_g \quad (1)$$

where $K$ is the thermal conductivity; $T$ is the temperature; $Q_g$ is the heating rate, which is zero in falling process; $\rho$, $C_p$ are the density and specific heat capacity separately.

In the transient process, the 10%-90% rising time $t_{up}$ and 90%-10% falling time $t_{down}$ can be described by the analytic formulas [5]:

$$t_{up} = \frac{2.2\rho C_p V}{1/R_{therm} - \alpha_{RTC} R_0 I^2} \quad (2)$$

$$t_{down} = 2.2\rho C_p V R_{therm} \quad (3)$$

where $V$ is the total volume of the heater, cladding and silicon waveguide; $R_0$ is the electric resistance at room temperature; $R_{therm}$ is the thermal resistance from waveguide to substrate,

978-1-7281-1647-1/19/$31.00 ©2019 IEEE

which is inversely proportional to the thermal conductivity ($K$) of waveguide and cladding; $I$ is the electric current of heater; $\alpha_{RTC}$ is the electric resistance temperature coefficient. It is observed from the (2) and (3) that the response times can be reduced by the decrease of the $\rho$, $C_p$, $V$ and the increase of $K$.

## III. Results and Discussion

### A. Effects of Layer Thickness on the Response Speed

Based on the above model and formulas, $t_{up}$ and $t_{down}$ with respect to Au thickness and $SiO_2$ cladding thickness are calculated and depicted in Fig. 2. The differences between the simulated and analytic results are smaller than 20%, indicating that they have high consistency. Because of the increasing volume when Au thickness rises from 0.08 µm to 0.16 µm and $SiO_2$ cladding thickness changes from 0.4 µm to 1.2 µm, $t_{up}$ and $t_{down}$ increase about 10% and 40%, respectively. Thus, increase of these thicknesses will decrease the response speed.

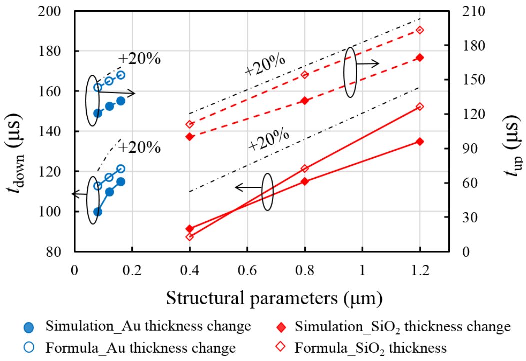


Fig. 2. Influences of Au layer thickness and $SiO_2$ cladding thickness on the falling time $t_{down}$ and rising time $t_{up}$

### B. Effects of Materials on the Response Speed

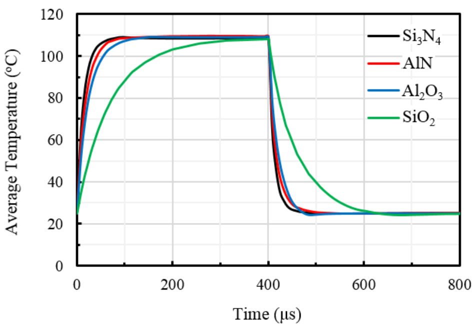


Fig. 3. Influences of cladding materials on the response time

Fig. 3 presents the simulated response process of cases with four cladding materials. It is evident that the response time can be largely reduced by more than 65% when the $SiO_2$ cladding is replaced by $Al_2O_3$, AlN and $Si_3N_4$ cladding. For example, $t_{up}$ of the $SiO_2$ case, the $Al_2O_3$ case, the AlN case and the $Si_3N_4$ case are 157.5 µs, 51.4 µs, 38.9 µs and 29.4 µs, respectively. Among these cases, the $Si_3N_4$ case has the highest response speed because of the high thermal conductivity and small heat capacity. Moreover, the calculating values of analytic formulas agree well with the simulation results, which have discrepancy of less than 20%.

## IV. Conclusion

The temperature response processes of thermally tunable devices have been simulated by transient model, and corresponding response speeds are optimized with the guidance of the analytic formulas. The results show that the response speed can be improved, either by reducing the thicknesses of metallic heater and cladding, or increasing the thermal conductivity of materials. The effects of materials on response speed are more apparent with normal layer thicknesses and cladding materials. Substituting the $SiO_2$ cladding by $Al_2O_3$, AlN and $Si_3N_4$ cladding, the response time can reduce more than 65%. These results demonstrate that the transient model and analytic formulas could be helpful for the design and optimization of thermally tunable devices with suspended waveguide.

## Acknowledgment

This work was supported in part by the National Natural Science Foundation of China (No. 61675073), in part by Fundamental Research Funds for the Central Universities (2016YXZD004), in part by the National High Technology Developing Program of China (2013AA014503), and in part by Wuhan International Joint Laboratory on Optoelectronics.

## Reference


[1] D. Dai, D. Liu, S. Wang, Reconfigurable Photonic Integrated Devices on Silicon, in *Nanophotonics and Micro/Nano Optics International Conference*, Proc. SPIE, pp. 1080230B: 1-10, October 2018.

[2] C.R. Raum, R. Gauthier, R.N. Tait, Integrated heaters for the thermal tuning of Bragg grating filters on silicon-on-insulator rib waveguides, *Microwave Opt. Technol. Lett.*, vol. 53, no. 3, pp. 672-676, March 2011.

[3] P.A. Cooper, L.G. Carpenter, C. Holmes, C. Sima, J.C. Gates, P.G.R. Smith, Power-efficiency enhanced thermally tunable Bragg grating for silica-on-silicon photonics, *IEEE Photonics J.*, vol. 7, no. 2, pp. 1-11, April 2015.

[4] P. Sun, R.M. Reano, Submilliwatt thermo-optic switches using free-standing silicon-on-insulator strip waveguides, *Opt. Express*, vol. 18, no. 8, pp. 8406-8411, April 2010.

[5] F. Duan, K. Chen, Y. Yu, Optimization of thermally tunable grating filters with air trench and beam-pillar structures, *Opt. Commun.*, vol. 439, pp. 239-243, May 2019.

[6] K. Chen, F. Duan, Y. Yu, High-performance thermo-optic tunable grating filters based on laterally supported suspended silicon ridge waveguide, *Opt. Express*, vol. 26, no. 15, pp. 19479-19488, July 2018.

[7] M. Asheghi, M.N. Touzelbaev, K.E. Goodson, Y.K. Leung, S.S. Wong, Temperature-dependent thermal conductivity of single-crystal silicon layers in SOI substrates, *J. Heat Trans.*, vol. 120, pp. 30-36, February 1998.

[8] T. Yamane, N. Nagai, S. Katayama, M. Todoki, Measurement of thermal conductivity of silicon dioxide thin films using a 3ω method, *J. Appl. Phys.*, vol. 91, pp. 9772-9776, June 2002.

[9] P. Qu, W. Chen, F. Li, C. Liu, W. Dong, Analysis and design of thermo-optical variable optical attenuator using three-waveguide directional couplers based on SOI, *Opt. Express*, vol. 16, no. 25, pp. 20334-20344, November 2008.

[10] C. Duquenne, M.P. Besland, P.Y. Tessier, E. Gautron, Y. Scudeller, D. Averty, Thermal conductivity of aluminium nitride thin films prepared by reactive magnetron sputtering, *J. Phys. D Appl. Phys.*, vol. 45, pp. 218-224, December 2012.

[11] A. Atabaki, E.S. Hosseini, A. Eftekhar, S. Yegnanarayanan, A. Adibi, Optimization of metallic microheaters for high-speed reconfigurable silicon photonics, *Opt. Express*, vol. 18, no. 17, pp. 18312-18323, August 2010.

[12] X. Han, Q. Cheng, F. Liu, Y. Yu, Numerical Analysis on Thermal Tuning Efficiency and Thermal Stress of a Thermally Tunable SG-DBR Laser, *IEEE Photonics J.*, vol. 8, no. 3, pp. 1-12, June 2016.